Peer-reviewed version available at Fibers 2018, 6, 74; doi:10.3390/fib6040074

*Article*

# Geometry of chalcogenide negative curvature fibers for $CO_2$ laser transmission

**Chengli Wei** [1], **Curtis R. Menyuk** [2] and **Jonathan Hu** [1,*]

[1] Department of Electrical and Computer Engineering, Baylor University, 76798 Waco, USA; jonathan_hu@baylor.edu

[2] Department of Computer Science and Electrical Engineering, University of Maryland Baltimore County, 21227 Baltimore, USA; menyuk@umbc.edu

* Correspondence: jonathan_hu@baylor.edu; Tel.: +1-254-710-1853

**Abstract:** We study impact of geometry on leakage loss in negative curvature fibers made with $As_2Se_3$ chalcogenide and $As_2S_3$ chalcogenide glasses for carbon dioxide ($CO_2$) laser transmission. The minimum leakage loss decreases when the core diameter increases both for fibers with six and for fibers with eight cladding tubes. The optimum gap corresponding to the minimum loss increases when the core diameter increases for negative curvature fibers with six cladding tubes. For negative curvature fibers with eight cladding tubes, the optimum gap is always less than 20 $\mu$m when the core diameter ranges from 300 $\mu$m to 500 $\mu$m. The influence of material loss on fiber loss is also studied. When material loss exceeds $10^2$ dB/m, it dominates the fiber leakage loss for negative curvature fiber at a wavelength of 10.6 $\mu$m.

**Keywords:** $CO_2$ lasers; negative curvature fibers; chalcogenide glass; fiber loss; mid-IR

## 1. Introduction

Carbon dioxide ($CO_2$) lasers have been widely used in surgery, medicine, and material processing [1–3]. Step index fibers are commonly used to transmit $CO_2$ laser light. The nonlinearity in the silica glass limits the transmitted power. Hollow-core fibers have low nonlinearity, because the light is mostly transmitted in air, which does not contribute to the nonlinearity. In addition, it is possible in principle to obtain a lower loss in hollow-core fiber than in step-index fiber because air does not contribute to material loss [4,5]. Recently, hollow-core negative curvature fibers have drawn a large amount of attention due to their attractive properties including low loss, broad bandwidth, and a high damage threshold [6–12]. The delivery of mid-infrared radiation has also been successfully demonstrated using chalcogenide negative curvature fibers for a $CO_2$ laser at a wavelength of 10.6 $\mu$m [13–15]. Previous study shows that chalcogenide glass should be used for wavelength larger than 4.5 $\mu$m [16]. The relative simplicity of the negative curvature structure could enable the fabrication of fiber devices for mid-IR applications using non-silica glasses, such as chalcogenide [13–15].

The guiding mechanism in negative curvature fibers is inhibited coupling [10,17,18]. A large amount of research [10,19] has been carried out to determine the impact of the fiber parameters on the leakage loss [20] in negative curvature fibers and then optimize these parameters to minimize the loss. These parameters include the curvature of the core boundary, the number of cladding tubes, the thickness of the tubes, and the nested cladding tubes [17,18,21–24]. By introducing a gap between cladding tubes, the loss can be decreased in negative curvature fibers [24,25]. When the tubes touch, modes exist in the localized node area. A separation between the cladding tubes removes the additional resonances due to the localized node. Fibers with a gap between tubes are also expected to be easier to fabricate, since surface tension would naturally assist to maintain the circular shape of the tubes [22]. On the other hand, when the gap is too big, the core mode can leak through the gaps, which increases the loss in negative curvature fibers [26]. Therefore, an optimum gap exists. The optimal gap corresponding to the minimum loss in a fiber with six cladding tubes is three times as large as

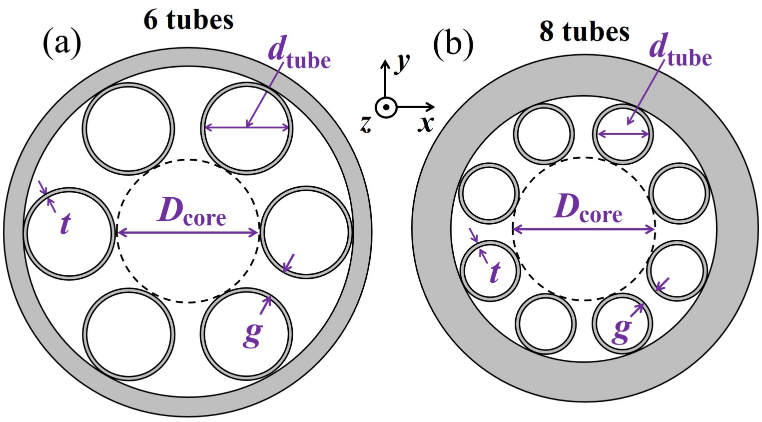


**Figure 1.** Schematic illustration of negative curvature fibers with (a) six and (b) eight cladding tubes.

the optimal gap in fibers with eight or ten cladding tubes [26]. A larger gap is required to remove the weak coupling between the core mode and tube modes in a fiber with six cladding tubes [26].

In this paper, we find optimal structures of chalcogenide negative curvature fibers for $CO_2$ laser transmission, in which we minimize the loss in the two-dimensional parameter space that consists of the core diameter and the gap size. In previous studies, the optimum gap was found in negative curvature fibers with a fixed core diameter [26]. We find that the minimum leakage loss decreases when the core diameter increases both for fibers with six and for fibers with eight cladding tubes. The optimum gap increases when the core diameter increases for negative curvature fibers with six cladding tubes. The optimum gap is always less than 20 $\mu$m when the core diameter increases for negative curvature fibers with eight cladding tubes when the core diameter ranges from 300 $\mu$m to 500 $\mu$m.

## 2. Geometry

Negative curvature fibers with six and eight cladding tubes have been fabricated by several research groups [17,25,27,28]. Figure 1 shows schematic illustrations of negative curvature fibers with six and eight cladding tubes. The gray regions represent glass, and the white regions represent air. The inner tube diameter, $d_{\text{tube}}$, the core diameter, $D_{\text{core}}$, the tube wall thickness, $t$, the minimum gap between the cladding tubes, $g$, and the number of tubes, $p$, are related by the expression: $D_{\text{core}} = (d_{\text{tube}} + 2t + g)\sin(\pi/p) - (d_{\text{tube}} + 2t)$ [29]. The wavelength of 10.6 $\mu$m for a $CO_2$ laser is used in our simulation.

## 3. $As_2Se_3$ chalcogenide glass

In this section, we study the loss in negative curvature fibers made with $As_2Se_3$ chalcogenide glass. The material loss of 10.6 dB/m for $As_2Se_3$ chalcogenide glass is included in the simulation [30]. The tube thickness, $t$, is fixed at 5.2 $\mu$m corresponding to the third antiresonance. A glass thickness corresponding to the third antiresonance has been drawn in the past [15]. We first study negative curvature fibers with six cladding tubes. We define $d_{6\text{max}}$ as the maximum possible tube diameter for the fiber with 6 cladding tubes, which equals $D_{\text{core}} - 2t$. Figure 2(a) shows the contour plot of loss as a function of core diameter, $D_{\text{core}}$, and normalized tube diameter, $d_{\text{tube}}/d_{6\text{max}}$. For a fixed $D_{\text{core}}$, the loss decreases and then increases when $d_{\text{tube}}/d_{6\text{max}}$ increases from 0.2 to 1.0. The minimum loss occurs when $d_{\text{tube}}/d_{6\text{max}}$ = 0.62, and it does not change when $D_{\text{core}}$ increases from 300 $\mu$m to 500 $\mu$m. The loss decreases when $D_{\text{core}}$ increases. In addition, we show the loss as a function of the core diameter, $D_{\text{core}}$, and the gap, $g$, in Fig. 2(b). The loss first decreases and then increases as the gap, $g$, increases. When there is no gap, a mode exists in the node that is created by the two touching tubes [25]. When the gap is too large, core mode leaks through the gap [17,26]. We also plot the loss as a function of gap, $g$, for

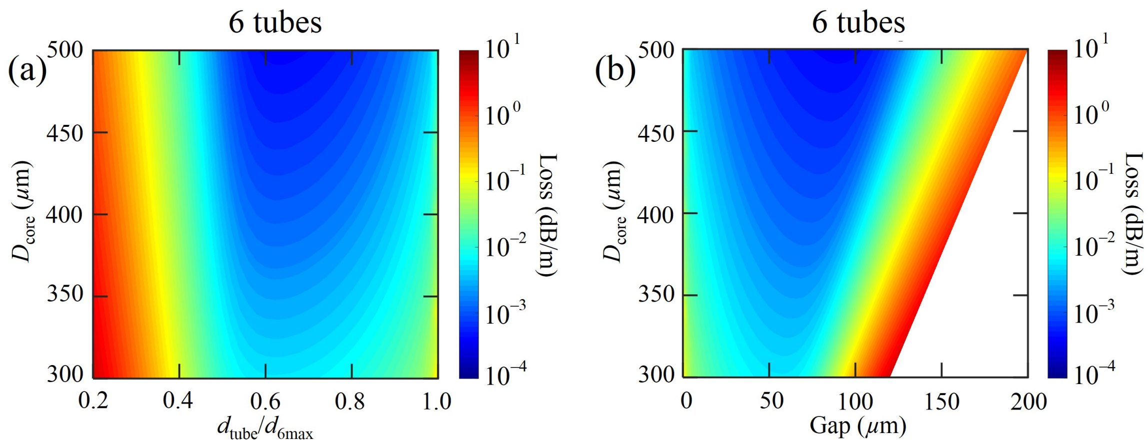


**Figure 2.** (a) Contour plot of loss as a function of core diameter and normalized tube diameter. (b) Contour plot of loss as a function of core diameter and gap. The number of cladding tube is six.

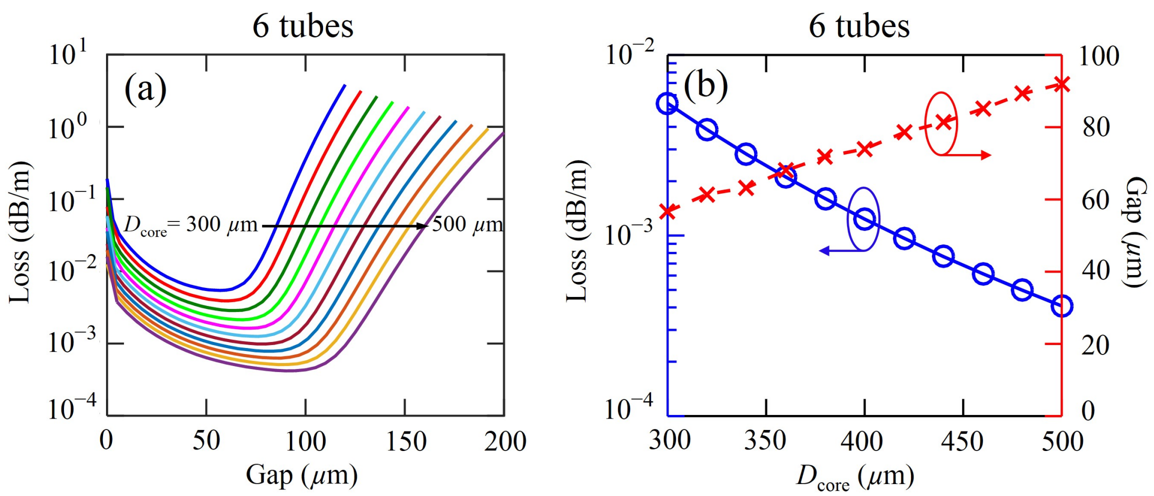


**Figure 3.** (a) Loss as a function of gap in fibers with different core diameters. (b) Minimum loss and the corresponding optimum gap in fibers with different core diameters. The number of cladding tube is six.

different core diameters in Fig. 3(a). In order to quantify the minimum loss and the corresponding optimum gap for different core diameters, we also plot the minimum loss and the corresponding optimum gap, $g$, using blue solid curve and red dashed curves, respectively, in Fig. 3(b). When the core diameter increases from 300 $\mu$m to 500 $\mu$m, the minimum loss decreases by more than one order of magnitude and the corresponding optimum gap, $g$, increases from 60 $\mu$m to 90 $\mu$m. Hence, a larger gap is needed for a fiber with a larger core diameter to lower the loss in negative curvature fibers with six cladding tubes.

We next carry out the same loss analysis on negative curvature fibers with eight cladding tubes. Figure 4(a) shows the contour plot of loss as a function of core diameter, $D_{\text{core}}$, and normalized tube diameter, $d_{\text{tube}}/d_{8\text{max}}$, where $d_{8\text{max}}$ is defined as the maximum possible tube diameter for the fiber with 8 cladding tubes, which is $\{D_{\text{core}}\sin(\pi/8) - 2t[1-\sin(\pi/8)]\}/[1-\sin(\pi/8)]$ [31]. Figure 4(b) shows the contour plot of loss as a function of core diameter, $D_{\text{core}}$, and gap, $g$. The minimum loss occurs at a larger value of $d_{\text{tube}}/d_{8\text{max}}$, or a smaller value of $g$, than is the case for negative curvature fibers with six cladding tubes. In Fig. 5(a), we show the loss as a function of the gap, $g$, for different

doi:10.20944/preprints201807.0263.v1

Peer-reviewed version available at Fibers 2018, 6, 74; doi:10.3390/fib6040074



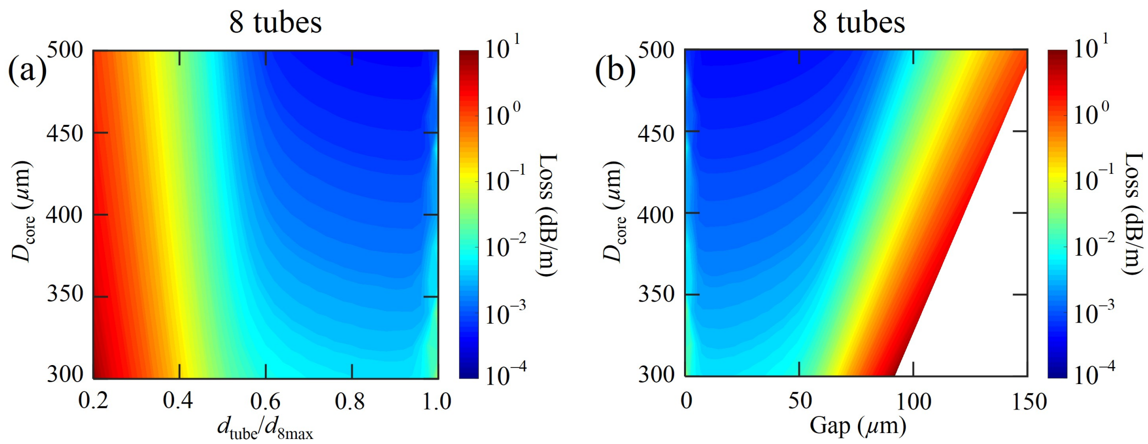


**Figure 4.** (a) Contour plot of loss as a function of core diameter and normalized tube diameter. (b) Contour plot of loss as a function of the core diameter and gap. The number of cladding tube is eight.

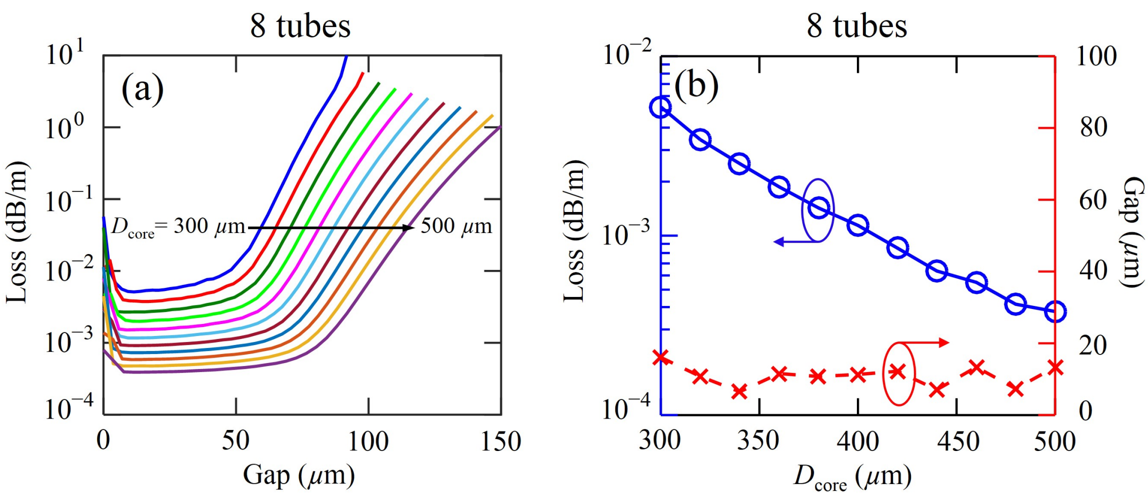


**Figure 5.** (a) Loss as a function of the gap in fibers with different core diameters. (b) Minimum loss and the corresponding gap in fibers with different core diameters. The number of cladding tubes is eight.

core diameters. The optimum gap corresponding to the minimum loss is less than 20 $\mu$m for fibers with different core diameters and the loss increases slowly when gap further increases. The minimum loss and the corresponding gap, $g$, are plotted using blue solid curve and red dashed curves, respectively, in Fig. 5(b). The minimum loss decreases by around one order of magnitude when the core diameter increases from 300 $\mu$m to 500 $\mu$m. Different from fibers with six cladding tubes, the corresponding optimum gap, $g$, is much smaller and is always less than 20 $\mu$m when the core diameter increases from 300 $\mu$m to 500 $\mu$m in fibers with eight cladding tubes. There is a wide range of gaps that realize low loss in the fibers with eight cladding tubes, as shown in Fig. 5(a). The loss is less sensitive to the gap in the region between 10 $\mu$m and 50 $\mu$m. Since the tube diameter is much smaller than the diameter of core, the coupling between the core mode and tube modes is weak. A larger gap is needed for fibers with six cladding tubes to remove the weak coupling between the core mode and cladding tube modes in negative curvature fibers with six cladding tubes.

Preprints (www.preprints.org) | NOT PEER-REVIEWED | Posted: 16 July 2018 doi:10.20944/preprints201807.0263.v1

Peer-reviewed version available at Fibers 2018, 6, 74; doi:10.3390/fib6040074



## 4. $As_2S_3$ chalcogenide glass

In this section, we carried out the same loss analysis in negative curvature fibers made with $As_2S_3$ chalcogenide glass. The material loss of 500 dB/m for $As_2S_3$ chalcogenide glass is included in the simulation [15,16]. The tube thickness, $t$, is fixed at 6.1 $\mu$m corresponding to the third antiresonance. Figure 6(a) shows the loss as a function of gap, $g$, when the core diameter increases from 300 $\mu$m to 500 $\mu$m in $As_2S_3$ chalcogenide fiber with six cladding tubes. Compared with the loss in Fig. 3(a), the losses in the fiber using $As_2S_3$ chalcogenide glass, shown in Fig. 6(a), are higher and have a flatter minimum. In Fig. 6(b), we show the minimum loss and the corresponding gap, $g$, as blue solid curve and red dashed curve, respectively. We also study the fiber leakage loss with and without material loss in an $As_2S_3$ chalcogenide fiber with six cladding tubes. In Fig. 7(a), we show the results in order to explain the broad, low-loss region in Fig. 6(a). The core diameter is fixed at 300 $\mu$m. The solid curve shows the fiber loss with material loss of 500 dB/m for $As_2S_3$ chalcogenide glass, which is the same as the blue solid curve in Fig. 6(a). The dashed curve shows the fiber loss without material loss, which is similar to the curve in Fig. 3(a). The high material loss of $As_2S_3$ chalcogenide glass dominates and leads to a flat minimum in the fiber loss curve, as shown by the blue solid curve in Fig. 7(a).

In order to better illustrate the influence of the material loss on the total fiber loss, we study the fiber loss as a function of material loss both for $As_2S_3$ chalcogenide glass and $As_2Se_3$ chalcogenide glass, shown in Fig. 7(b) as the red dashed and blue solid curves, respectively. The core diameter is 300 $\mu$m and the gap is 60 $\mu$m. The fiber loss changes little when the material loss increases from 0.1 dB/m to 10 dB/m, and the fiber loss is dominated by the confinement loss in the blue region for both curves. The loss of fiber that is made with $As_2Se_3$ chalcogenide glass is located in the blue region, which is marked with the blue circle on the blue solid curve. The fiber loss begins to increase when the material loss increases from 10 dB/m to $10^2$ dB/m, and the influence of the material loss becomes visible. When the material loss further increases, the fiber loss increases sharply, and the fiber loss is dominated by the material loss in the red region for both curves, when the material loss is higher than $10^2$ dB/m. The loss of fiber made with $As_2S_3$ chalcogenide glass is located in the red region, which is marked with the red triangle on the red dashed curve.

Figure 8(a) shows the loss as a function of gap, $g$, in $As_2S_3$ chalcogenide fiber with eight cladding tubes. In Fig. 8(b), we show the minimum loss and the corresponding gap, $g$, using a blue solid curve and a red dashed curve, respectively. The minimum loss decreases by less than one order of magnitude and the corresponding optimum gap, $g$, is always less than 20 $\mu$m, which agrees with the results in the

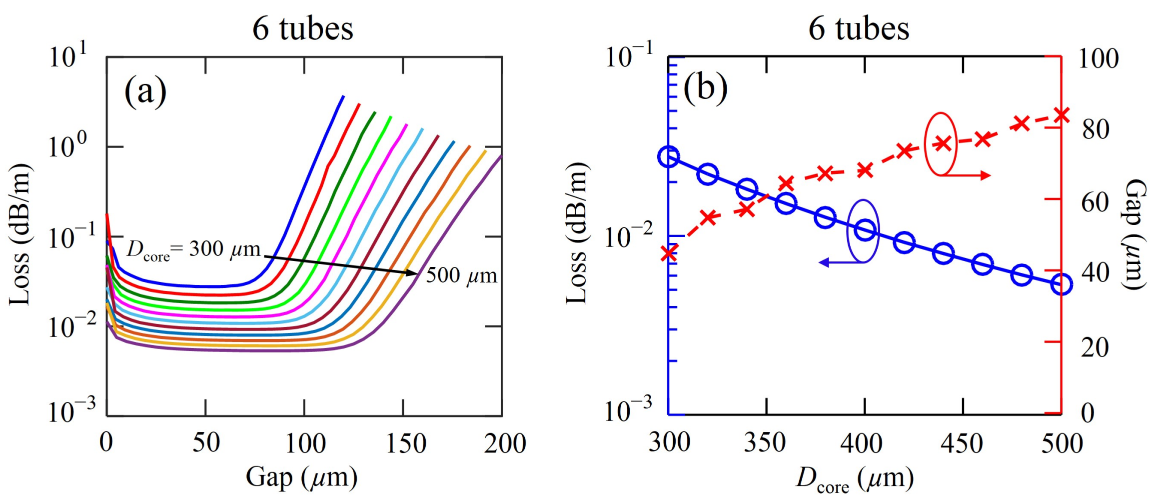


**Figure 6.** (a) Loss as a function of gap in fibers with different core diameters. (b) Minimum loss and corresponding optimum gap in fibers with different core diameters. There are six cladding tubes.

Preprints (www.preprints.org) | NOT PEER-REVIEWED | Posted: 16 July 2018 doi:10.20944/preprints201807.0263.v1

Peer-reviewed version available at Fibers 2018, 6, 74; doi:10.3390/fib6040074



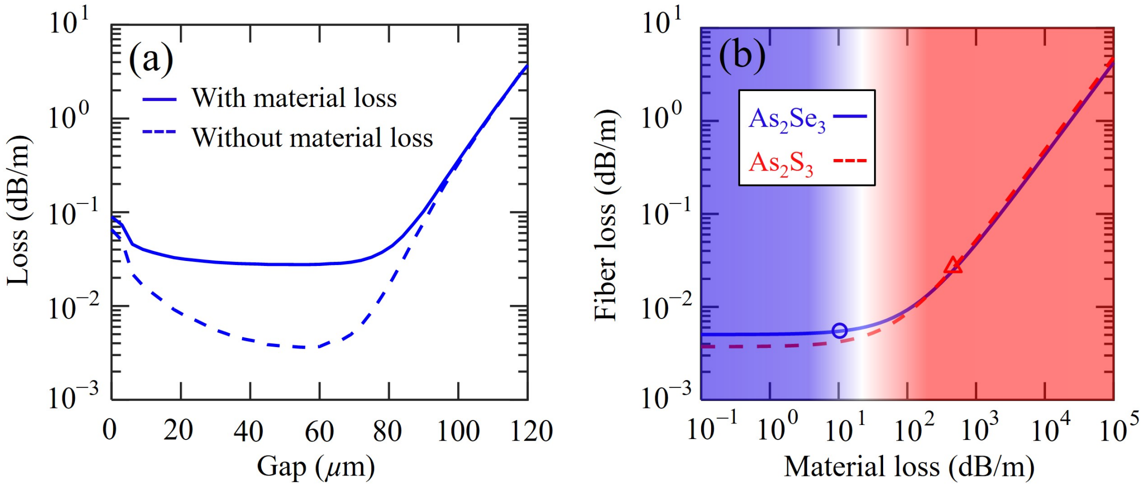


**Figure 7.** (a) Loss as a function of gap in fibers with and without material loss. (b) Fiber loss as a function of material loss in $As_2Se_3$ chalcogenide glass fiber and $As_2S_3$ chalcogenide glass fiber with six cladding tubes, a core diameter of 300 $\mu$m, and a gap of 60 $\mu$m.

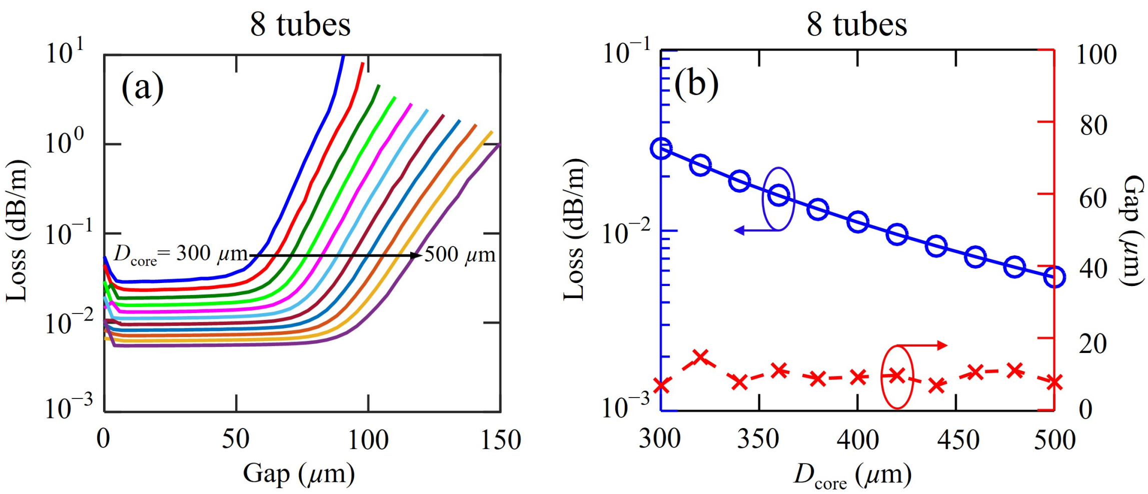


**Figure 8.** (a) Loss as a function of gap in fibers with different core diameters. (b) Minimum loss and corresponding gap in fibers with different core diameters. The number of cladding tube is eight.

$As_2Se_3$ chalcogenide fiber with 8 cladding tubes. Small loss variation near zero gap occurs due to the glass modes existed near the node area between two tubes in Fig. 8(a).

## 5. Conclusions

In this paper, we optimize the structure of negative curvature fibers for $CO_2$ laser transmission. We investigate the impact of the size of the gap between cladding tubes on the loss of negative curvature fibers made with $As_2Se_3$ and $As_2S_3$ chalcogenide glasses. For $As_2Se_3$ chalcogenide fibers with six cladding tubes, the minimum loss decreases by an order of magnitude and the corresponding optimum gap, $g$, increases from 60 $\mu$m to 90 $\mu$m when the core diameter increases from 300 $\mu$m to 500 $\mu$m. A greater gap is needed for a fiber with greater core diameter to reduce the coupling between the core mode and tube mode. For a fiber with eight cladding tubes, the optimum gap, $g$, that corresponds to the minimum loss is always less than 20 $\mu$m when the core diameter ranges from 300 $\mu$m to 500 $\mu$m. We also study $As_2S_3$ chalcogenide fibers, which has a higher material loss at a wavelength of 10.6 $\mu$m. It is found that material loss dominates the fiber leakage loss. The fiber loss is dominated by the material loss, when the material absorption loss is higher than $10^2$ dB/m.

**Author Contributions:** Supervision, Curtis Menyuk and Jonathan Hu; Validation, Curtis Menyuk and Jonathan Hu; Writing – original draft, Chengli Wei; Writing – review & editing, Chengli Wei, Curtis Menyuk and Jonathan Hu.

**Conflicts of Interest:** The authors declare no conflict of interest.

## References

1. Snakenborg, D.; Klank, H.; Kutter, J. P. Microstructure fabrication with a $CO_2$ laser system. *J. Micromech. Microeng.* **2004**, *14*, 182–189.
2. Hædersdal, M.; Sakamoto, F.H.; Farinelli, W.A.; Doukas, A.G.; Tam, J.; Anderson, R.R. Fractional $CO_2$ laser-assisted drug delivery. *Lasers Surg. Med.* **2010**, *42*, 113–122.
3. Witteman, W.J. In *The $CO_2$ Laser*; Enoch, J.F., Macadam, D.L., Schawlow, A.L., Shimoda, K., Tamir, T.; Springer-Verlag: Berlin, Germany, 1987; pp. 1–4, ISBN 978-3-540-47744-0.
4. Poletti, F.; Petrovich, M.N.; Richardson, D. J. Hollow-core photonic bandgap fibers: technology and applications. *Nanophotonics* **2013**, *2*, 315–340.
5. Roberts, P.J.; Couny, F.; Sabert, H.; Mangan, B.J.; Williams, D.P.; Farr, L.; Mason, M.W.; Tomlinson, A.; Birks, T.A.; Knight, J.C.; Russell. P.St.J. Ultimate low loss of hollow-core photonic crystal fibres. *Opt. Express* **2005**, *13*, 236–244 .
6. Wang, Y.; Couny, F.; Roberts, P.J.; Benabid. F. Low loss broadband transmission in optimized core-shaped Kagome hollow-core PCF. In Proceedings of the Lasers Electro-Optics, Quantum Electron, Laser Science Conference, San Jose, CA, USA, 16–21 May 2010; paper CPDB4.
7. Wang, Y.Y.; Wheeler, N.V.; Couny, F.; Roberts, P.J.; Benabid, F. Low loss broadband transmission in hypocycloid-core Kagome hollow-core photonic crystal fiber. *Opt. Lett.* **2011**, *36*, 669–671.
8. Pryamikov, A.D.; Biriukov, A.S.; Kosolapov, A.F.; Plotnichenko, V.G.; Semjonov, S.L.; Dianov, E. M. Demonstration of a waveguide regime for a silica hollow-core microstructured optical fiber with a negative curvature of the core boundary in the spectral region >3.5 $\mu$m. *Opt. Express* **2011**, *19*, 1441–1448 .
9. Yu, F.; Wadsworth, W. J.; Knight. J. C. Low loss silica hollow core fibers for 3–4 $\mu$m spectral region. *Opt. Express* **2012**, *20*, 11153–11158.
10. Wei, C.; Weiblen, R. J.; Menyuk, C. R.; Hu, J. Negative curvature fibers. *Adv. Opt. Photon.* **2017**, *9*, 504–561.
11. Michieletto, M.; Lyngs, J.K.; Jakobsen, C.; Lgsgaard, J.; Bang, O.; Alkeskjold, T.T. Hollow-core fibers for high power pulse delivery. *Opt. Express* **2016**, *24*, 7103–7119.
12. Wei, C; Menyuk, C. R.; Hu, J. Polarization-filtering and polarization-maintaining low-loss negative curvature fibers. *Opt. Express* **2018**, *26*, 9528–9540.
13. Kosolapov, A.F.; Pryamikov, A.D.; Biriukov, A.S.; Shiryaev, V.S.; Astapovich, M.S.; Snopatin, G.E.; Plotnichenko, V.G.; Churbanov, M.F.; Dianov, E.M. Demonstration of $CO_2$-laser power delivery through chalcogenide glass fiber with negative-curvature hollow core. *Opt. Express* **2011**, *19*, 2572–25728.
14. Shiryaev, V.S. Chalcogenide glass hollow-core microstructured optical fibers. *Front. Mater.* **2015**, *2*, 24.
15. Gattass, R.R.; Rhonehouse, D.; Gibson, D.; McClain, C.C.; Thapa, R.; Nguyen, V.Q.; Bayya, S.S.; Weiblen, R.J.; Menyuk, C.R.; Shaw, L.B.; Sanghera, J.S. Infrared glass-based negative-curvature anti-resonant fibers fabricated through extrusion. *Opt. Express* **2016**, *14*, 25697–25703 .
16. Wei, C.; Hu, J.; Menyuk, C.R. Comparison of loss in silica and chalcogenide negative curvature fibers as the wavelength varies. *Front. Phys.* **2016**, *4*, 30.
17. Debord, B.; Amsanpally, A.; Chafer, M.; Baz, A.; Maurel, M.; Blondy, J. M.; Hugonnot, E.; Scol, F.; Vincetti, L.; Gérôme, F.; Benabid, F. Ultralow transmission loss in inhibited-coupling guiding hollow fibers. *Optica* **2017**, *4*, 209–217 .
18. Debord, B.; Alharbi, M.; Bradley, T.; Fourcade-Dutin, C.; Wang, Y.Y.; Vincetti, L.; Gérôm, F.; Benabid, F. Hypocycloid-shaped hollow-core photonic crystal fiber Part I: arc curvature effect on confinement loss. *Opt. Express* **2013**, *21*, 28597–28608.
19. Yu, F.; Knight, J. C. Negative curvature hollow-core optical fiber. *IEEE J. Sel. Top. Quantum Electron.* **2016**, *22*, 4400610.

Peer-reviewed version available at *Fibers* **2018**, *6*, 74; doi:10.3390/fib6040074



20. Hu, J.; Menyuk, C. R. Understanding leaky modes: slab waveguide revisited. *Adv. Opt. Photon.* **2009**, *1*, 58–106.
21. Alagashev, G.K.; Pryamikov, A.D.; Kosolapov, A.F.; Kolyadin, A.N.; Lukovkin, A.Y.; Biriukov, A.S. Impact of geometrical parameters on the optical properties of negative curvature hollow core fibers. *Laser Phys.* **2015**, *25*, 055101.
22. Poletti, F. Nested antiresonant nodeless hollow core fiber. *Opt. Express* **2014**, *22*, 23807–23828.
23. Habib, M.S.; Bang, O.; Bache, M. Low-loss hollow-core silica fibers with adjacent nested anti-resonant tubes. *Opt. Express* **2015**, *23*, 17394–17406.
24. Belardi, W.; Knight, J. C. Hollow antiresonant fibers with reduced attenuation. *Opt. Lett.* **2014**, *39*, 1853–1856.
25. Kolyadin, A.N.; Kosolapov, A.F.; Pryamikov, A.D.; Biriukov, A.S.; Plotnichenko, V.G.; Dianov, E.M. Light transmission in negative curvature hollow core fiber in extremely high material loss region. *Opt. Express* **2013**, *21*, 9514–9519.
26. Wei, C.; Menyuk, C.R.; Hu, J. Impact of cladding tubes in chalcogenide negative curvature fibers. *IEEE Photon. J.* **2016**, *8*, 2200509.
27. Uebel, P.; Günendi, M. C., Frosz, M.H.; Ahmed, G.; Edavalath, N. N.; Ménard, J.-M.; Russell, P. St.J. Broadband robustly single-mode hollow-core PCF by resonant filtering of higher-order modes. *Opt. Lett.* **2016**, *41*, 1961–1964.
28. Liu, X.; Ding, W.; Wang, Y. Y.; Gao, S.; Cao, L.; Feng, X.; Wang, P. Characterization of a liquid-filled nodeless anti-resonant fiber for biochemical sensing. *Opt. Lett.* **2017**, *42*, 863–866.
29. Wei, C; Menyuk, C.R.; Hu, J. Bending-induced mode non-degeneracy and coupling in chalcogenide negative curvature fibers. *Opt. Express* **2016**, *24*, 12228–12239.
30. Caillaud, C.; Renversez, G.; Brilland, L.; Mechin, D.; Calvez, L.; Adam, J.-L.; Troles, J. Photonic Bandgap Propagation in All-Solid Chalcogenide Microstructured Optical Fibers. *Materials* **2014**, *7*, 6120–6129.
31. Wei, C; Kuis, R.A.; Chenard, F; Menyuk, C.R.; Hu, J. Higher-order mode suppression in chalcogenide negative curvature fibers. *Opt. Express* **2015**, *23*, 15824–15832.